New Journal of Physics
The open access journal at the forefront of physics

Deutsche Physikalische Gesellschaft DPG IOP Institute of Physics

PAPER • OPEN ACCESS

Vacuum-ultraviolet laser source for spectroscopy of trapped thorium ions

To cite this article: J Thielking *et al* 2023 *New J. Phys.* **25** 083026

IOP Publishing New J. Phys. 25 (2023) 083026 https://doi.org/10.1088/1367-2630/aced1b

New Journal of Physics
The open access journal at the forefront of physics

Deutsche Physikalische Gesellschaft DPG
IOP Institute of Physics

Published in partnership with: Deutsche Physikalische Gesellschaft and the Institute of Physics

OPEN ACCESS

RECEIVED
15 April 2023

REVISED
18 July 2023

ACCEPTED FOR PUBLICATION
3 August 2023

PUBLISHED
14 August 2023

PAPER

Vacuum-ultraviolet laser source for spectroscopy of trapped thorium ions

J Thielking, K Zhang, J Tiedau, J Zander[1], G Zitzer, M V Okhapkin and E Peik[*]

Physikalisch-Technische Bundesanstalt, Bundesallee 100, 38116 Braunschweig, Germany
[1] Present address: Institut für Laserphysik und Zentrum für Optische Quantentechnologien, Universität Hamburg, Hamburg, Germany.
[*] Author to whom any correspondence should be addressed.

E-mail: ekkehard.peik@ptb.de

Keywords: VUV laser, trapped ions, nuclear laser excitation

Abstract

A tunable vacuum-ultraviolet (VUV) laser source based on four-wave frequency mixing in xenon is presented. Using seed radiation from two continuous-wave lasers, the system allows for precise control of the VUV frequency and is developed for the resonant laser excitation of the Th-229 nucleus to its low-energy isomeric state. The system is prepared to operate in a wide scanning range from 148 nm to 155 nm. The source produces pulses of 6–10 ns duration with up to 40 μJ energy and is coupled via a vacuum beamline to a linear radiofrequency ion trap. In a first implementation of VUV laser spectroscopy of trapped Th^+ ions we excite three previously unknown resonance lines near 149 nm wavelength to electronic levels that are close to the Th-229 isomer energy. The resonances are detected and analyzed via fluorescence of the excited Th^+ ions. An analysis of the lineshape is used to estimate the linewidth of the VUV radiation to be in the range of $\leqslant$6 GHz, dominated by phase noise that is enhanced in harmonic generation and in the four-wave mixing process. The prospects for the use of the system in nuclear laser spectroscopy of Th-229 are discussed.

1. Introduction

The low energy of about 8 eV above the ground state makes the ^{229}Th isomeric state accessible to laser excitation, but the experimental realization of this phenomenon remains a demanding challenge. Direct laser excitation of the thorium isomer is a complex task because of the significant uncertainty in the nuclear transition wavelength lying in the vacuum ultraviolet range (VUV) around 150 nm and because of challenges in the development of the laser radiation sources in this range [1]. Since suitable nonlinear optical crystals for frequency conversion from continuous-wave (CW) lasers are not available for this wavelength range, harmonic generation from femtosecond frequency combs [2, 3], and four-wave-mixing (FWM) conversion of pulsed laser radiation [4–6] in gases are considered as the most promising light sources for the laser excitation of the isomeric state in ^{229}Th.

A pulsed VUV radiation source using resonance-enhanced four-wave difference mixing in xenon gas can provide high-intensity pulses of tunable VUV light from 122 nm (10.2 eV) to 168 nm (7.4 eV) [7]. The VUV radiation pulse power of the source is in the range of 10^{13} photons per 6–10 ns pulse for the wavelengths 150–160 nm. Typical power spectral densities obtained in four-wave mixing experiments are in the range of 1 pW Hz^{-1}. The spectral brightness of such a VUV source is quite high for the energy range of the thorium isomer, making four-wave difference mixing in xenon a useful tool for nuclear laser spectroscopy of ^{229}Th.

Here we present a VUV laser source based on four-wave difference mixing in xenon. The source is developed for the spectroscopy of trapped thorium ions and we demonstrate the excitation of three electronic transitions in $^{232}Th^+$ in the range of the nuclear isomer energy. The experiment allows us to characterize the VUV source for laser spectroscopy and demonstrates that the source can be used for the excitation of the isomer in ^{229}Th. We note that there is also considerable interest in laser excitation of trapped ions of other elements in this wavelength range, for example for proposed optical clocks with Pb^{2+} [8] and Sn^{2+} [9] or for laser cooling of Al^+ [10]. Similar techniques like the ones demonstrated here may be employed in those cases.

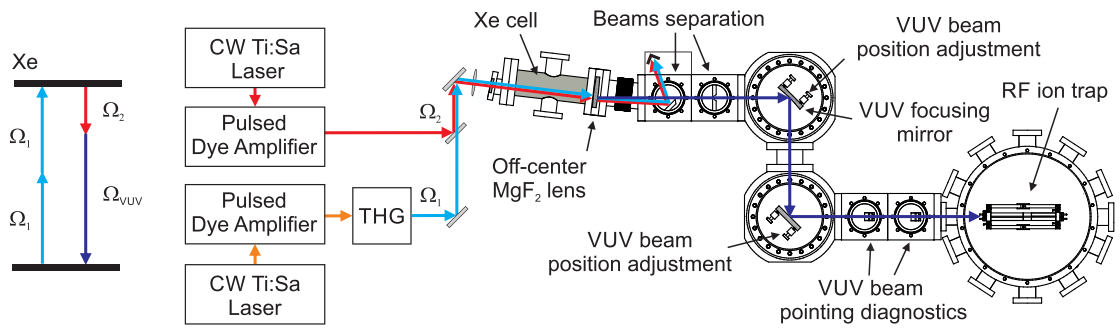

Figure 1. Schematics of the VUV source based on resonance-enhanced four-wave difference mixing in xenon gas for laser excitation of trapped Th^+ ions.

2. Experimental apparatus

The experimental setup for the VUV laser excitation of thorium is shown schematically in figure 1. It consists of two CW Ti:sapphire ring lasers with two pulsed dye amplification stages, a frequency tripling unit (THG), a Xe gas cell for the four-wave mixing, an ultra-high vacuum VUV beam line, a radio-frequency (RF) ion trap [11], and thorium spectroscopy diode lasers (not shown in figure 1, see [11, 12]).

The VUV radiation is generated in the Xe cell by resonance-enhanced four-wave mixing at the frequency $\Omega_{\mathrm{VUV}} = 2 \times \Omega_1 - \Omega_2$ (see, for example [7, 13–15]). Two Ti:sapphire CW lasers (MBR-110, Coherent and Matisse 2 TR, Sirah Lasertechnik) are used as seed lasers for the pulsed dye amplifiers. The frequency of the first CW Ti:sapphire laser is stabilized to excite, after frequency tripling, the two-photon resonance $5p^6\,{}^1S_0 \rightarrow 5p^5({}^2P^{\circ}_{3/2})6p\,{}^2[{}^1/_2](J=0)$ of Xe at 80 119 cm^{-1} $(2 \times \Omega_1)$. The corresponding fundamental wavelength is 748.8 nm. The second CW Ti:sapphire laser is tunable and provides a wavelength in the range from 765 nm to 800 nm to define the difference frequency (Ω_2) of the four-wave mixing process [4].

The two amplifiers (PulsedAmp 5x, Sirah Lasertechnik) are pumped by one lamp-pumped pulsed laser (SpitLight 2000, InnoLas Laser) with a repetition rate of 30 Hz, a pulse energy of 1 J at 532 nm, and a pulse duration of $\approx$ 10 ns. The amplifiers are operated using the laser dyes Styryl 8 (LDS 751) and Styryl 11 (LDS 798), generating laser pulses with a typical energy of 50 mJ and 25 mJ, respectively. Both amplifiers incorporate a stimulated Brillouin scattering (SBS) cell to suppress amplified spontaneous emission. These cells cause a negative frequency shift of the output radiation with respect to the seed laser of about 2 GHz. This shift is taken into account for all frequencies given in this paper. The output beam of the first amplifier is frequency tripled using two barium borate (BBO) crystals in a single pass configuration. The first BBO crystal generates the second harmonic (SHG) at 374.4 nm of the amplifier output radiation. The SHG radiation is then separated from the fundamental radiation using a dichroic mirror. Its polarization is rotated by 90° using a half-wave-plate, before recombining it with the fundamental beam. SHG and fundamental radiation are then converted to 249.6 nm (Ω_1) in the second BBO crystal. The half-wave-plate enables us to optimize the frequency tripling, achieving an output energy of 4 mJ per pulse at Ω_1.

Both amplified laser beams at frequencies Ω_1 and Ω_2 are expanded with telescopes with an expansion ratio of 1:1.5 and 1:1.2, respectively, before being combined with a dichroic mirror and focused into the Xe cell using an achromatic objective consisting of a fused silica lens and a MgF_2 lens. These telescope expansion ratios are selected to achieve beam waists for the UV and IR radiation in the focal point of $\leqslant 100\,\mu$m. The waists of the two beams are measured using the knife-edge technique.

At the exit of the Xe cell an off-axis MgF_2 lens ($f = 150$ mm) is used to split the co-linear VUV, UV, and IR radiation [16]. The diameter of the lens is 50 mm and the off-axis displacement is about 15 mm. The separated UV and IR beams are reflected to a beam block using a D-shaped mirror. To keep the VUV radiation deflection angle constant over the frequency tuning range, the position of the MgF_2 lens can be shifted perpendicular to the incoming propagation of the laser beams. The VUV beam is passed through a 3 mm wide slit milled in a ceramic plate to reduce residual stray light from the UV/IR beams in the direction of the experiment. The ceramic plate is mounted on a linear translation stage allowing the slit to be moved in and out of the VUV beam.

A Ce:YAG scintillator crystal is mounted on the same plate next to the slit for visual inspection of the VUV beam position. The scintillator emission is detected with a CMOS camera. Two more Ce:YAG scintillators are mounted on translation stages further along the beam line to provide a visual control of the VUV radiation.

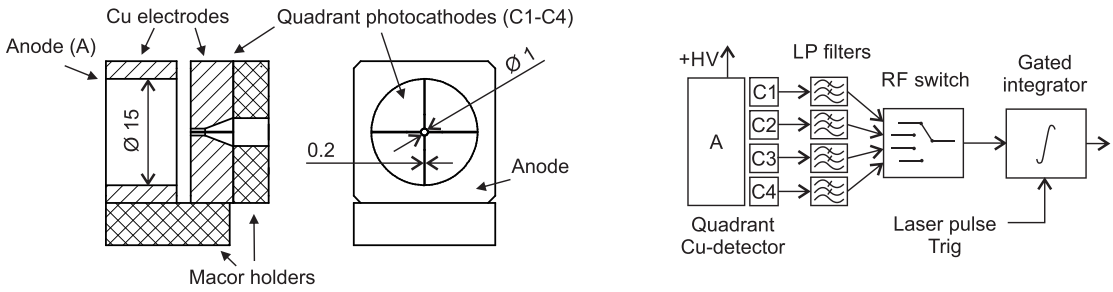

Figure 2. Design of the quadrant photo-electron detectors and readout electronics for VUV beam alignment.

The beam can be steered to pass through the ion trap center using two high-reflective mirrors, each mounted on a motorized mirror holder. The first mirror has a concave shape ($R \approx 1200\,\text{mm}$) to create a focal point close to the trap center.

To ensure the correct beam alignment, two precision beam position detectors are used in our system. In analogy to quadrant photodiodes used for detecting the position of laser beams, we developed quadrant detectors based on the photo-electric effect (see, for example, [17, 18]). Each consists of four copper photocathodes (C1–C4) and a common copper ring anode (A) (figure 2). The detectors are mounted on *XZ* vacuum manipulators and a central hole with a diameter of 1 mm serves for the initial position adjustment of the detector in the vacuum chamber to a reference laser beam. During operation, electrons are ejected from the photocathodes when exposed to the VUV beam, since the energy of incident VUV photons exceeds the work function of copper. The ejected electrons are then collected by the anode, which has a potential of $+300\,\text{V}$ applied to it. The photo-currents of the individual photocathodes are converted to voltage using $50\,\Omega$ resistors and smoothed using low pass filters with a cutoff frequency of 15 MHz. The four signals are then applied in repeated sequence to a gated integrator (SRS SR250) using an RF switch. The gated integrator output signal is in turn read out in the same sequence by a computer program. The signals are converted to an absolute beam position, which provides feedback to the motorized mirror holders to adjust the beam to the centers of both detectors.

To measure the VUV pulse energy, we use a vacuum-compatible pyroelectric detector (PEM 24 VUV, SLT Sensor- und Lasertechnik). The detector is mounted to the side of the beam line, separated from it with a CaF_2 viewport, and individually evacuated. The VUV beam can be directed toward the detector with a mirror mounted at 45° incident angle on a translation stage, which is located directly in front of the ion trap chamber.

3. Operation and characterization of the VUV source

The 1σ-uncertainty range of the presently most accurate wavelength determination for the ^{229}Th nuclear transition reaches from 148.27 nm to 149.13 nm [19]. We therefore optimize the VUV laser system in this wavelength range for the highest possible pulse energy, while maintaining the ability to scan over a wider range with the same set of parameters. The highest mean power over the frequency scanning range is achieved at a xenon pressure of 500 Pa and a detuning of $2\Omega_1$ from the two-photon resonance of 150 GHz, obtaining up to 27 μJ of VUV pulse energy. A limiting factor is the xenon resonance line $5p^6\,{}^1S_0 \rightarrow 5p^5({}^2P^\circ_{3/2})6s\,{}^2[3/2]^\circ (J=1)$ at 146.96 nm, causing a loss of phase matching for higher pressures when approaching this wavelength.

For further optimization of the laser parameters for the latest predicted thorium isomer wavelength we investigate the relation between the generated VUV pulse energy and the pulse energies of the UV and IR beams (figure 3). To this end, we reduce the UV pulse energy by reducing the THG efficiency using the aforementioned half-wave plate. The UV and VUV pulse energies are recorded while the IR pulse energy is kept constant at 16 mJ (figure 3(a)). In a second measurement, the UV power is kept at 3 mJ while the IR power is reduced by reducing the pump power of the pulsed amplifier using a polarizer (figure 3(b)).

The observed linear relation between VUV and UV pulse energies differs from the expected quadratic dependency of a two-photon transition. This can be caused by an intensity-dependent loss of Xe atoms through photo-ionization, leading to a saturation of the four-wave-mixing process [13, 14]. The linear dependency between VUV and IR power is expected due to the single IR photon in the FWM process, indicating no saturation with respect to the IR pulse energy in this range.

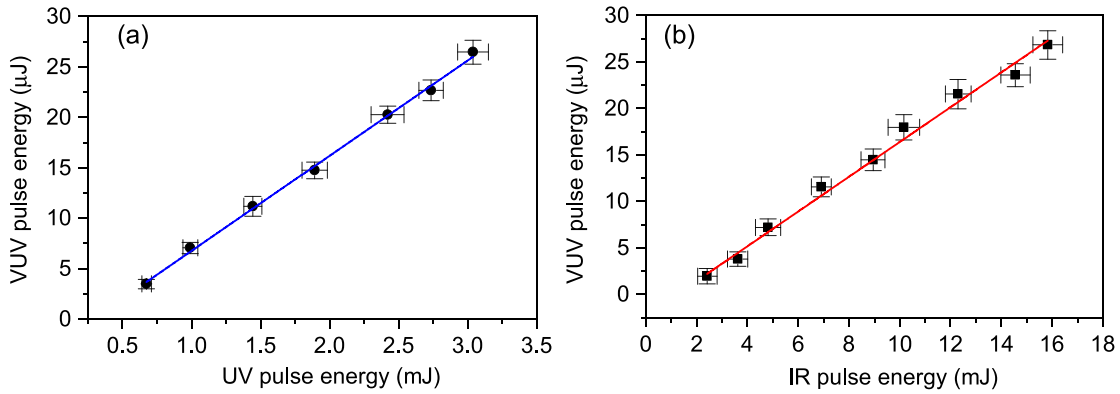

Figure 3. VUV pulse energy as a function of (a) UV and (b) IR pulse energy. The straight lines are drawn to guide the eye.

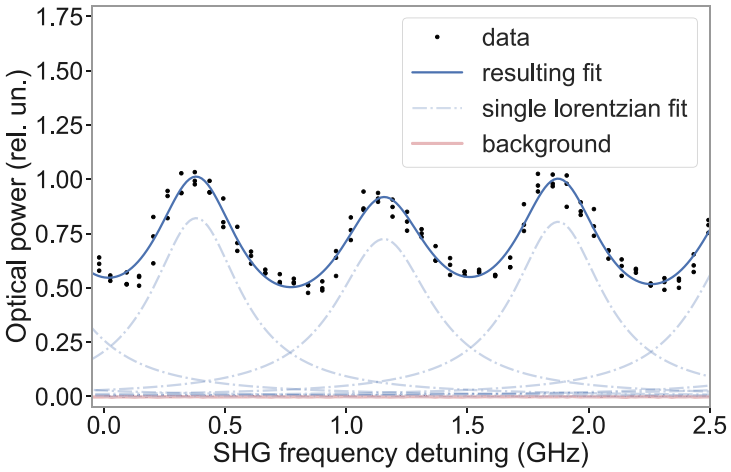

Figure 4. Cavity transmission resonances of the second harmonic radiation at 374.4 nm.

To reach an extended scanning range including previously predicted values for the isomer energy, we also investigated a laser configuration using a DCM dye amplifier and a difference photon wavelength of 650 nm to generate 155 nm radiation. VUV pulse energies of up to 40 μJ were achieved with 2 kPa xenon pressure. By reaching 40 μJ VUV pulse energy an appearance of a saturation effect is observed at the IR pulse energy $>$30 mJ. With an appropriate selection of dyes the tuning range from 150 nm to 155 nm can be covered with a nearly constant power level [7].

We also investigate the linewidth of the VUV radiation, since the excitation rate of the nuclear transition in the upcoming experiments is determined by the spectral brightness of the VUV source. For an initial lower limit estimation we measure the linewidth of the two amplifiers by coupling their output radiation to a confocal cavity with a free spectral range of 1.5 GHz. Both amplifiers show a linewidth of $\approx$200 MHz, close to the Fourier limit set by the pulse duration and in agreement with the specifications given by the manufacturer. We assume that the third harmonic generation inserts the main contribution to the linewidth of the VUV source. The expected linewidth of the VUV source can be estimated from the linewidth of the amplifier using the enhancement factor of 3^2 for the spectral density of the THG radiation (see, for example [20]) and the additional enhancement factor of 2 due to the two-photon excitation in Xe. The radiation of the second amplifier used for difference-frequency generation also affects the VUV line. Therefore, the expected linewidth of the VUV source is approximately 4 GHz.

To estimate the broadening effects, we measure the linewidth of the second harmonic radiation at 374.4 nm generated in the frequency tripler using a second confocal cavity with a free spectral range of 1.5 GHz. The record of the cavity transmission signal is shown in figure 4. The cavity signal demonstrates transmission resonances on the top of a significant offset which indicates the presence of phase noise in the radiation spectra of the second harmonic. Therefore, the phase noise conversion yields an additional broadening of the amplifier linewidth. However, the cavity measurement does not allow us to derive the phase noise pedestal width due to its non-Lorentzian shape and the relatively small cavity free spectral range.

Assuming an unknown conversion of phase noise and no background signal on the detector, we fitted a sequence of Lorentzian functions to the recorded transmission signal. The best fit shows a linewidth of ≈450 MHz at 374 nm. However, this can only be assumed as a lower limit due to the unresolved phase noise contribution. In order to determine the effective linewidth of the FWM radiation source in the VUV range we perform spectroscopic investigations of $^{232}Th^{+}$ resonance lines as described in the following section.

4. VUV spectroscopy of trapped Th^{+} ions

High-lying electronic states of Th^{+} in the range of the nuclear excitation energy have already been investigated with laser spectroscopy in [21]. Only states of even parity were addressed because a two-step excitation scheme from the even parity electronic ground state was used. In contrast, the VUV excitation reported here addresses electronic states of odd parity with single photon transitions, which have so far not been known in this energy range. We therefore employ a wide scanning of the VUV source in the range around 148 nm to search for electronic states. Spectroscopy via fluorescence detection is combined with the detection of resonance-enhanced ionization to Th^{2+} in order to clearly identify these transitions. The width of the resonances is used to determine the linewidth of the VUV radiation.

4.1. Spectroscopy setup

For the VUV excitation of thorium ions we use a linear Paul trap as described in [11]. The trap is loaded with Th^{+} ions by ablating a metallic thorium target using a pulsed Nd:YAG laser and it has the capacity to store about 10^{6} $^{232}Th^{+}$ ions. Using argon buffer gas at 0.1 Pa pressure, we cool the ions to room temperature and depopulate metastable states via collisional quenching [11]. The 4th harmonic radiation at 266 nm of a Q-switched solid-state laser with a pulse energy of ≈20 μJ and 1 kHz repetition rate is used for photodissociation of molecular Th^{+} compounds that form in reactions with impurities in the buffer gas [22]. The operation parameters of the ion trap allow to store both singly and doubly charged thorium ions simultaneously or to make it stable only for Th^{+}.

Figure 5 shows a simplified partial level scheme and the transitions relevant to our investigations. The amount of trapped Th^{+} ions is monitored by laser excitation and fluorescence detection of the strong resonance line at 402 nm, using a diode laser in ECDL configuration. In our previous experiments with two-photon excitation of high-lying levels in Th^{+} [22] we observed the appearance of Th^{2+} ions correlated with the fluorescence decay signal of Th^{+} as a result of resonantly enhanced multi-photon ionization. Because our VUV source provides even higher pulse power we expect the appearance of two-photon ionization via a high-lying electronic state in parallel with the single photon excitation of the level. We therefore also monitor the trapped $^{232}Th^{2+}$ amount using a second ECDL at 459 nm to excite the 21 784 cm^{-1} level. The radiation of both ECDLs is aligned counter-propagating to the VUV beam. Pulses of the lasers are formed by acousto-optic modulators at a repetition rate of 1020 Hz, chosen as a multiple of the VUV repetition frequency. The same repetition rate is chosen for the photo-dissociation laser. The excitation pulse of the 402 nm laser diode is shifted in time from the VUV pulse to ensure that the VUV interacts with the Th^{+} ions predominantly in their ground state. Nevertheless a non-vanishing population of lower-lying states is present [11, 21, 22].

The fluorescence of the excited thorium ions is detected using three photomultiplier tubes (PMTs) with different spectral responses. Two PMTs with narrowband filters are used to determine the amount of Th^{+} and Th^{2+} ions and a broadband third PMT is used to detect the fluorescence during the VUV excitation. It is equipped with a long pass filter (300 nm cut off wavelength) blocking VUV and UV photons, since the stray light during the intense VUV pulse would saturate the PMT. Fast gated integrators and gated photon counters are used to evaluate the PMT signals during selected detection windows.

4.2. Spectroscopic signals

While scanning the VUV source in the range between 148.2 nm and 149.0 nm we observe three transitions from the ground state to high-lying states in Th^{+} (see table 1).

For all three transitions, the fluorescence decay signal of the high-lying Th^{+} states is accompanied by two-photon ionization for high VUV pulse energies. However, the ionization process almost vanishes for low VUV pulse energies. Figure 6(a) shows a typical fluorescence signal of a high-lying state with a resonance full widths at half maximum of 13 GHz. The signal is observed with the relevant PMT during the detection window overlapped with the VUV pulses. Figure 6(b) shows the decrease of the fluorescence signal of the 24 874 cm^{-1} level in Th^{+} due to two-photon ionization during the VUV scan. The 402 nm radiation pulse is used for the excitation of the 0 $cm^{-1} \rightarrow$ 24874 cm^{-1} transition in Th^{+} (see figure 5). After passing the minimum, the fluorescence signal slightly increases again due to a redistribution of singly and doubly charged ions in the trap. The two-photon ionization is also detected by the excitation of the

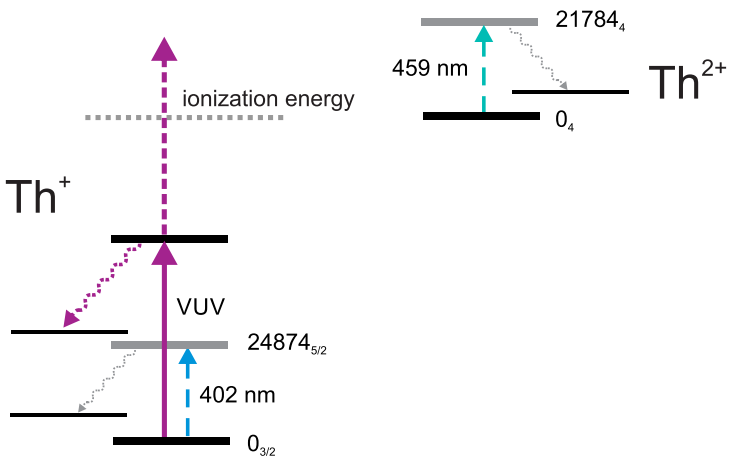

Figure 5. Partial level schemes of Th^+ and Th^{2+}, showing the employed transitions for excitation and fluorescence detection. The Th^+ transition at 402 nm and the Th^{2+} transition at 459 nm are used to detect the number of trapped ions in one charge state or the other.

Table 1. Newly observed odd-parity Th^+ levels. The uncertainty consists of statistical contributions from the fits and systematic shifts of the wavelength meter used in the experiment.

Excitation wavelength	Level
148.8122(5) nm	67 198.8(2) cm^{-1}
148.6675(5) nm	67 264.2(2) cm^{-1}
148.2033(5) nm	67 474.9(2) cm^{-1}

0 cm^{-1} → 21784 cm^{-1} transition in Th^{2+} at 459 nm. The fluorescence decay signal of the 21 784 cm^{-1} level is shown in figure 6(c). The signal represents the number of doubly ionized ions in the ion trap. The fluorescence does not remain constant after reaching the maximum, but decreases in time because of the formation of Th^{2+} molecular compounds.

To exclude a possible misclassification of the signal that we associate with Th^{2+}, it was verified that the signal is absent when the trap is operated with parameters making it unstable for Th^{2+}. Possible excitations from low-lying metastable states in Th^+ were excluded by changing the delay between the VUV pulse and the 402 nm pulse. Since the 402 nm pulse causes the population of low-lying metastable states, overlapping it with the VUV pulse would enlarge the fluorescence signal for transitions starting from these levels. On the other hand, the fluorescence signal of transitions starting from the ground state will be reduced due to the depopulation of the ground state by the 402 nm pulse.

4.3. Spectroscopic determination of the linewidth of the VUV source

Several broadening effects have to be subtracted from the measured widths of the VUV excitation spectra to get an estimation of the VUV source linewidth. Since the ions are only cooled with room temperature buffer gas they exhibit Doppler broadening. The actual mean ion temperature is measured by determining the linewidth of the 402 nm transition in Th^+ by scanning the frequency of the corresponding ECDL. The measured Doppler broadened linewidth is ≈1 GHz, corresponding to a temperature of ≈800 K and a Doppler broadening of 2.7 GHz in the VUV range. We therefore subtract 2.7 GHz from the observed resonance width to remove the contribution from Doppler broadening.

By solving dynamic rate equations for the levels involved in the excitation process, we have identified that the excitation rate is likely to be saturated for the peak radiation intensities during the VUV pulse. This saturation is also accompanied by power broadening of the fluorescence decay signal and by significant two-photon ionization. We therefore provide measurements with different VUV pulse energies to analyze the contribution of these effects.

Figure 7 shows the power broadening of the resonances for two VUV transitions from the ground state to the 67 199 cm^{-1} and 67 475 cm^{-1} states in Th^+. In these measurements the VUV pulse energy is reduced in two different ways. In one set the pulsed pump laser power is reduced by changing its internal Q-switch delay. In the other set only the pump power to the IR amplifier was reduced by using a polarizer. The linewidths that are observed with both methods are in agreement. A minimum resonance width of ≈ 6 GHz is obtained for the 67 199 cm^{-1} transition. Unfortunately, we cannot reduce the VUV pulse energy further

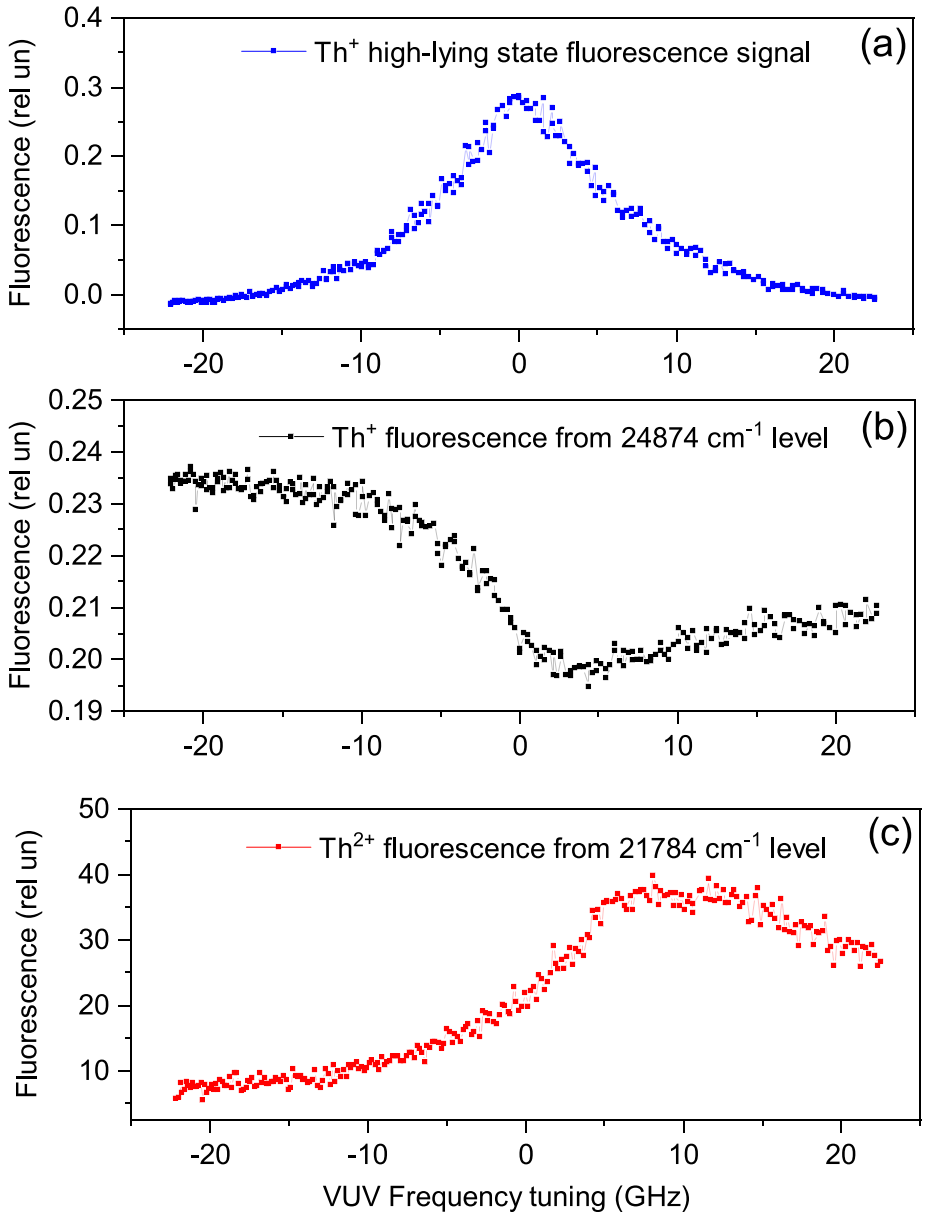

Figure 6. Typical fluorescence signals while scanning the VUV radiation frequency over the Th^+ resonance. Graph (a) shows the fluorescence decay of a high-lying state observed during the VUV pulse. Graph (b) shows the decrease of the fluorescence signal of Th^+ from the 24 874 cm^{-1} level due to two-photon ionization. Graph (c) demonstrates the build-up of Th^{2+} observed in the fluorescence from the decay of the 21 784 cm^{-1} level.

due to unstable operation of the amplifiers at low pump powers and a limited sensitivity of the in-vacuum VUV pulse energy detector.

In a further measurement, we reduce the VUV pulse energy by reducing the conversion efficiency of the third harmonic generation that produces the 249.6 nm beam. This is done by turning the half-wave plate after the SHG stage. In this case we observe a minimum width of the resonance of 10 GHz. Figure 8 shows the difference of the observed resonance width for the same VUV power obtained by reduction of the pump laser power and by tuning the THG efficiency. A Lorentzian function is fitted to both resonances to derive the broadening due to the difference in the linewidth of the VUV source. This shows that the width of the observed resonances is not only determined by power broadening but also by the linewidth of the VUV source. This in turn can be attributed to the third harmonic conversion of the amplifier phase and frequency noise. Most likely, for an optimal THG adjustment the laser emission peak is converted with higher efficiency with respect to the broadband noise pedestal which decreases the VUV linewidth.

Because the lifetime of the high-lying state is unknown, we assume that the broadening is fully determined by our VUV source. The linewidth of the source is therefore estimated as $\leqslant$6 GHz for the optimal adjustment of the third harmonic generation efficiency. By the reduction of the frequency tripler

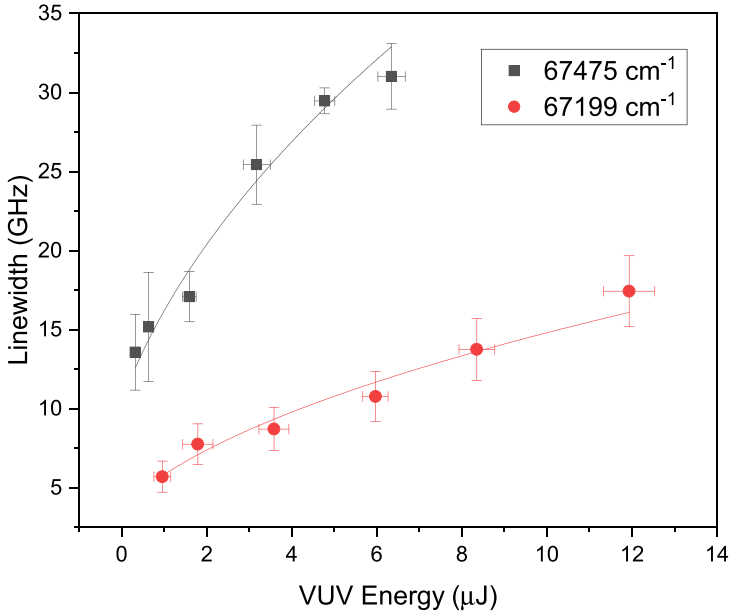

Figure 7. Width of the resonances vs. VUV pulse energy for two transitions. A contribution from Doppler broadening of 2.7 GHz is subtracted from the observed resonance widths.

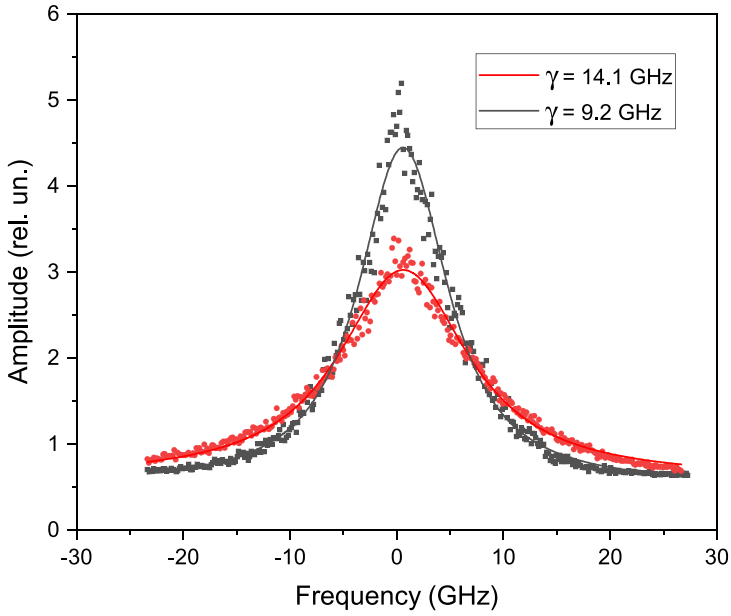

Figure 8. Line shape of the 67 199 cm^{-1} resonance for two different settings of the THG conversion efficiency, influencing the UV photons, for identical low VUV pulse energy of 1.8 μJ. Black data points correspond to the optimum tripler efficiency and the VUV pulse energy is adjusted with the pump laser delay or IR difference laser pump power. The red points are obtained at higher pump power but with a reduced conversion efficiency in the tripler.

conversion efficiency the linewidth of the VUV source becomes broader by a few GHz (the broadening lies within $\leqslant$5 GHz range).

5. Conclusions

A VUV source based on resonance-enhanced four-wave difference frequency mixing in xenon gas has been developed for the spectroscopy of thorium ions. The photon spectral density obtained in our experiment for the newly measured thorium isomer energy range is about 10^5 photons s^{-1} Hz^{-1}, which corresponds to a spectral power density of 0.1 pW Hz^{-1}. Because of the high spectral brightness, this VUV source is a useful tool for spectroscopy of Th in RF ion traps as well as for solid-state spectroscopy in Th-doped crystals [1].

We have measured the energies of three previously unknown high-lying electronic levels of odd parity in the energy range of 8.3 eV in $^{232}Th^{+}$.

Finally, we discuss an estimate of a direct excitation rate of the ^{229}Th isomeric state that can be expected with the VUV source presented here. Assuming that the spectral photon density of the VUV source is on the order of 10^5 photons s^{-1} Hz^{-1} and the beam waist is 100 μm, the excitation rate of the Th isomeric state can be estimated (see, for instance, Hilborn [23]) to be about 10^{-7} s^{-1} for each ion. Given the amount of about 10^4 thorium ions in the RF trap, it would take approximately thousand seconds to excite one thorium ion to the isomeric state. The present uncertainty range of the isomer energy [19] is still quite large for such an experiment and requires considerable scanning time. To improve the excitation rate of the isomeric state we are planning to increase the VUV power spectral density of the source by generating higher UV pulse energy from the third harmonics generation stage.

The spectroscopy of Th-doped crystals seems to be more promising for an initial VUV laser excitation of the isomer transition. The number of thorium nuclei in Th doped crystals is many orders of magnitude higher (up to 10^{18}) than in the trapped ion approach [24, 25]. Therefore we have implemented an additional VUV optical port in the vacuum system behind the ion trap vacuum chamber to combine both experiments, allowing us to perform spectroscopy experiments with trapped ions and Th-doped crystals at the same time.

Data availability statement

The data that support the findings of this study are openly available at the following URL/DOI: 10.5281/zenodo.8220302.

Acknowledgments

We would like to thank Thomas Leder and Martin Menzel for the design and manufacture of the mechanical structures. This work has been funded by the European Research Council (ERC) under the European Union's Horizon 2020 research and innovation programme (Grant Agreement No. 856415), the Deutsche Forschungsgemeinschaft (DFG) - SFB 1227 - Project-ID 274200144 (Project B04), and by the Max-Planck-RIKEN-PTB-Center for Time, Constants and Fundamental Symmetries.

References

[1] Beeks K, Sikorsky T, Schumm T, Thielking J, Okhapkin M V and Peik E 2021 *Nat. Rev. Phys.* **3** 238
[2] Gohle C, Udem T, Hermann M, Rauschenberger J, Holzwarth R, Schuessler H A, Krausz F and Hänsch T W 2005 *Nature* **436** 234
[3] Jones R J, Moll K D, Thorpe M J and Ye J 2005 *Phys. Rev. Lett.* **94** 193201
[4] Bjorklund G C 1975 *IEEE J. Quantum Electron.* **QE11** 287
[5] Hilbig R and Wallenstein R 1982 *Appl. Opt.* **21** 913
[6] Hollenstein U, Palm H and Merkt F 2000 *Rev. Sci. Instrum.* **71** 4023
[7] Hanna S J, Campuzano-Jost P, Simpson E A, Robb D B, Burak I, Blades M W, Hepburn J W and Bertram A K 2009 *Int. J. Mass Spectrom.* **279** 134
[8] Beloy K 2021 *Phys. Rev. Lett.* **127** 013201
[9] Leibrandt D R, Porsev S G, Cheung C, Safronova M S 2022 Prospects of a thousand-ion Sn^{2+} Coulomb-crystal clock with sub-10^{-19} inaccuracy (arXiv:2205.15484)
[10] Yu N, Dehmelt H and Nagourney W 1992 *Proc. Natl Acad. Sci. USA* **89** 7289
[11] Herrera-Sancho O A, Okhapkin M V, Zimmermann K, Tamm C, Peik E Taichenachev A V, Yudin V I and Głowacki P 2012 *Phys. Rev.* A **85** 033402
[12] Müller R A *et al* 2018 *Phys. Rev.* A **98** 020503(R)
[13] Hager J and Wallace S C 1982 *Chem. Phys. Lett.* **90** 472
[14] Hutchinson M H R and Thomas K J 1983 *IEEE J. Quantum Electron.* **19** 1823
[15] Hilbig R, Hilber G, Lago A, Wolff B and Wallenstein R 1986 *Proc. SPIE* **613** 49
[16] VonDrasek W A, Okajima S and Hessler J P 1989 *Appl. Opt.* **27** 4057
[17] Lee P, Gernhardt J, Armontrout C J and Snider R T 1988 *Rev. Sci. Instrum.* **59** 883
[18] Jeet J 2018 Search for the low lying transition in the 229Th Nucleus *UCLA Electronic Theses and Dissertations*
[19] Kraemer S *et al* 2023 *Nature* **617** 706–10
[20] Stein S R 1985 Frequency and time - their measurement and characterization *Precision Frequency Control* vol 2, ed E A Gerber and A Ballato (Academic Press)
[21] Meier D-M, Thielking J, Głowacki P, Okhapkin M V, Müller R A, Surzhykov A and Peik E 2019 *Phys. Rev.* A **99** 052514
[22] Herrera-Sancho O A, Nemitz N, Okhapkin M V and Peik E 2013 *Phys. Rev.* A **88** 012512
[23] Hilborn R C 1982 *Am. J. Phys.* **50** 982
[24] Kazakov G A, Litvinov A N, Romanenko V I, Yatsenko L P, Romanenko A V, Schreitl M, Winkler G and Schumm T 2012 *New J. Phys.* **14** 083019
[25] Beeks K *et al* 2023 *Sci. Rep.* **13** 3897